Analysis of Coexistence between IEEE 802.15.4, BLE and IEEE 802.11 in the 2.4 GHz ISM Band

Radhakrishnan Natarajan*†, Pouria Zand*, Majid Nabi†
*Holst Centre / IMEC-NL, High Tech Campus 31, 5656 AE Eindhoven, The Netherlands
†Department of Electrical Engineering, Eindhoven University of Technology, 5600 MB Eindhoven, The Netherlands
Email: *†r.natarajan@student.tue.nl, *pouria.zand@imec-nl.nl, †m.nabi@tue.nl

***Abstract*—The rapid growth of the Internet-of-Things (IoT) has led to a proliferation of low-power wireless technologies. A major challenge in designing an IoT network is to achieve coexistence between different wireless technologies sharing the unlicensed 2.4 GHz ISM spectrum. Although there is significant literature on coexistence between IEEE 802.15.4 and IEEE 802.11, the coexistence of Bluetooth Low Energy (BLE) with other technologies remains understudied. In this work, we examine coexistence between IEEE 802.15.4, BLE and IEEE 802.11, which are widely used in residential and industrial wireless applications. We perform a mathematical analysis of the effect of cross-technology interference on the reliability of the affected wireless network in the physical (PHY) layer. We also set up and perform PHY layer experiments to verify the analytical results. Finally, we extend the study to the Medium Access Control (MAC) layer. Our findings show that, even though the MAC layer mechanisms of IEEE 802.15.4 and BLE improve reliability, cooperative solutions are required to achieve coexistence.**

I. Introduction

In recent years, the emergence of IoT has led to an explosive growth in the number of smart wireless devices. Many IoT applications have their own Quality-of-Service (QoS) requirements. In response, various low-power wireless technologies such as IEEE 802.15.4 [1] and BLE [2] have been developed and adopted widely. The globally allowable operational band for these technologies is the unlicensed 2.4 GHz ISM band as shown in Fig. 1, which is also used by other wireless technologies such as IEEE 802.11 [3]. The result is cross-technology interference that affects the QoS of the network, particularly its reliability and latency, which may in turn lead to application failure. Achieving coexistence of different wireless technologies is therefore a major challenge in designing an IoT network.

Coexistence between different wireless technologies can be classified into three domains: space, time and frequency. Coexistence can thus be achieved by meeting one or more of the following conditions:

1) Adequate spacing between the networks
2) Controlled time-sharing of the channel
3) Adequate frequency separation between the networks

Coexistence mechanisms can be classified into two categories: non-cooperative and cooperative, depending on whether the involved networks operate independently of one another or coordinate their use of the spectrum. In non-cooperative coexistence, each network treats the other networks present as interference and performs interference mitigation. In cooperative coexistence, all the networks collaborate and coordinate their use of the spectrum in a fair way. An example use case of cooperative coexistence is a smart gateway that coordinates spectrum usage between multiple networks that employ different wireless technologies.

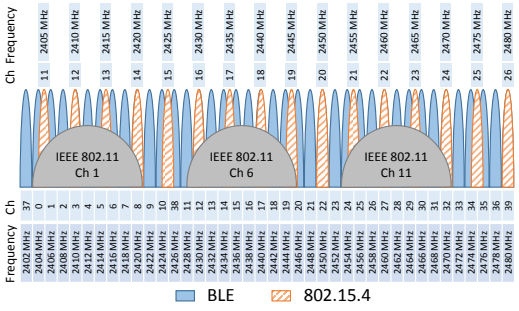

Fig. 1. 2.4 GHz ISM band: IEEE 802.15.4, BLE and IEEE 802.11 channels

In order to propose a coexistence solution for a given application, it is first necessary to study the effect of cross-technology interference on the performance of the involved wireless technologies. While existing studies in this topic area provide an insight into the nature of the coexistence issue, they fail to systematically analyse the effect of cross-technology interference. As a result, the outcomes are quite inconclusive and sometimes even contradictory. Furthermore, no research on coexistence between IEEE 802.15.4, BLE and IEEE 802.11 has yet been undertaken, even though these technologies are widely used in smart homes, smart buildings and industrial wireless applications.

To try and fill this knowledge gap, we perform a systematic analysis of coexistence between IEEE 802.15.4, BLE and IEEE 802.11b. The choice of IEEE 802.11b is arbitrary; this study can also be applied to other variants of IEEE 802.11. The contributions of this work can be summarised as follows:

1) Adopting the coexistence methodology introduced in [4] and applying it to IEEE 802.15.4, BLE and IEEE 802.11b
2) Performing a mathematical analysis to study PHY layer coexistence of these technologies and verifying the analytical results through experiments
3) Studying MAC layer coexistence through experiments
4) Providing a basis to connect this study to real-world application requirements

978-1-5090-3474-1/16/$31.00 ©2016 IEEE

The remainder of this paper is organised as follows. Section II discusses some of the existing literature on coexistence. Section III describes the mathematical analysis. Section IV discusses the outcomes of our experiments. Section V discusses the findings of our study. Section VI presents our conclusions. Finally, Section VII discusses the premises of this study as well as the scope for future work.

II. Related Work

There is a significant amount of literature available on coexistence between IEEE 802.15.4 and IEEE 802.11. Likewise, the coexistence of Bluetooth Classic [5] with other technologies has been studied extensively. However, the coexistence of BLE with other technologies remains understudied.

IEEE 802.15.2-2003 [6] specified recommended practices for coexistence of IEEE 802.15 Wireless Personal Area Networks (WPANs) with other networks operating in the same unlicensed frequency bands. The IEEE 802.19 Wireless Coexistence Working Group has extended this scope by developing standards for coexistence between wireless technologies in the unlicensed frequency bands. Their contributions to the field included a coexistence methodology [4], which analytically estimates the effect of cross-technology interference on the reliability of networks.

R. G. Garroppo et al. [7] researched the effect of IEEE 802.11 and Bluetooth Classic interference on IEEE 802.15.4 and vice versa through experiments. They found that the Packet Error Rate (PER) of IEEE 802.15.4 drops by around 40% due to IEEE 802.11 interference and by less than 10% due to Bluetooth Classic interference. Moreover, IEEE 802.15.4 is more affected by the distance to the IEEE 802.11 interferer than Bluetooth Classic. They also observed negligible effects on IEEE 802.11 or Bluetooth Classic, due to interference from IEEE 802.15.4.

S. Silva et al. [8] studied the effect of IEEE 802.11, IEEE 802.15.4 and Bluetooth Classic interference on BLE through experiments. They observed no effect on the PER and the Received Signal Strength Indicator (RSSI) of BLE as a result of interference from any of the other technologies. This indicates that frequency hopping in BLE is very effective in interference-avoidance.

J. Wyffels et al. [9] researched the interference effect of BLE advertising beacons on IEEE 802.11 through experiments. They observed that the impact of interference is significantly shaped by channel separation. At a channel separation of 70 MHz, they observed practically no impact on IEEE 802.11 traffic, whereas at 1 MHz, they observed a drop of around 50% in IEEE 802.11 throughput.

The existing coexistence studies in literature as discussed above, provide a limited analysis of the effect of interference. Furthermore, the results obtained are rather inconclusive. To try and bridge this gap, we set out to perform a systematic study of coexistence through both mathematical analysis and experiments. Furthermore, we study coexistence between IEEE 802.15.4, BLE and IEEE 802.11, which is of interest to residential and industrial wireless applications.

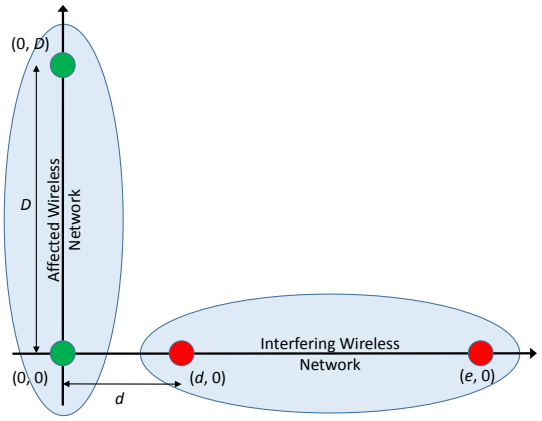

Fig. 2. Geometric model from [4]

III. Mathematical Analysis

In our mathematical analysis of coexistence, we adopt the methodology developed in [4] to estimate the PER caused by cross-technology interference, and apply it to IEEE 802.15.4, BLE and IEEE 802.11b. This PER estimate can be used to estimate other performance metrics such as latency and throughput. To make this paper self-contained and to ensure continuity, we include the derivation of the generic methodology from [4] here, and discuss how we apply it to these technologies. In this analysis, we consider only the PHY layers of the involved wireless technologies. The effect of MAC layer mechanisms is considered in the experimental study discussed in Section IV.

A. Methodology

The methodology developed in [4] takes the geometric model of the Affected Wireless Network (AWN) and the Interfering Wireless Network (IWN) as its starting point. Following this, a path-loss model is used to calculate the average Signal-to-Interference Ratio (SIR) at the AWN receiver, reflecting the signal and interference transmit powers and the geometry of the networks. A PHY layer model is then used to calculate the Symbol Error Rate (SER) of the AWN as a function of the SIR at the AWN receiver, assuming continuous interference. Finally, a temporal model takes into account the dynamic nature of the interference by modelling it as a pulse generator with known statistical properties, and calculates the AWN's PER as a function of SER.

We analyse the following four network configurations:

1) AWN = IEEE 802.15.4, IWN = BLE
2) AWN = IEEE 802.15.4, IWN = IEEE 802.11b
3) AWN = BLE, IWN = IEEE 802.15.4
4) AWN = BLE, IWN = IEEE 802.11b

B. Geometric model

The geometric model describes the location of the nodes of the AWN and the IWN. We consider the simple configuration proposed in [4] shown in Fig. 2, where each network consists of only two nodes. A more complex geometric model could

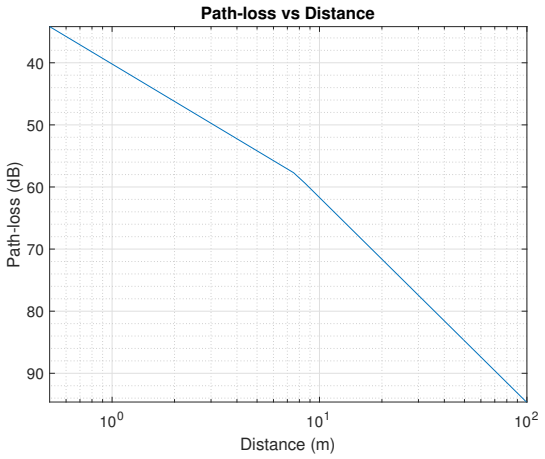

Fig. 3. Path-loss model from [6]

be used to study more realistic networks. It is further assumed that only one IWN node is near the AWN, focusing only on the interference caused by that node on the AWN. In order to study the worst case interference during unidirectional transfer, we assume the node at $(0, 0)$ to be the receiver, the node at $(0, D)$ to be the transmitter and the node at $(d, 0)$ to be the interferer. The same geometric model is used for all four network configurations.

C. Path-loss model

The distances in the geometric model are translated into signal attenuation using the path-loss model. The path-loss model is chosen depending on the frequency band used and the environment the networks operate in. We use the path-loss model recommended in [6] for indoor environments in the 2.4 GHz band. It is a piecewise linear model, described by Eqn. 1 and shown in Fig. 3, that represents free-space path-loss up to 8 m, and a more cluttered environment beyond 8 m.

$$pl(d) = \begin{cases} 40.2 + 20 \cdot log_{10}(d) & 0.5m < d \leq 8m \\ 58.5 + 33 \cdot log_{10}(d/8) & d > 8m \end{cases} \quad (1)$$

Using the geometry of Fig. 2, the SIR, γ, at the receiver is calculated as follows. First, the signal and interference powers at the receiver, $P^r_{S,dB}$ and $P^r_{I,dB}$, are calculated using the well-known path-loss formula, given the transmitted signal and interference powers, $P^t_{S,dB}$ and $P^t_{I,dB}$, and the corresponding distances, D and d.

$$\begin{aligned} P^r_{S,dB} &= P^t_{S,dB} - pl(D) \\ P^r_{I,dB} &= P^t_{I,dB} - pl(d) \end{aligned} \quad (2)$$

Following this, the interference power after the receiver filter, P^{rf}_I, is calculated depending on the relative bandwidths of the interferer, B_I, and the receiver filter, B_F, as discussed in [4].

$$P^{rf}_I = \begin{cases} P^r_I & B_I \leq B_F \\ P^r_I B_F / B_I & B_I > B_F \end{cases} \quad (3)$$

The occupied signal bandwidth of IEEE 802.15.4 is 2 MHz, of BLE is 1 MHz, and of IEEE 802.11b is 22 MHz. IEEE 802.15.4 and BLE have a receiver filter bandwidth of 2 MHz. P^{rf}_I is therefore calculated accordingly for the four network configurations.

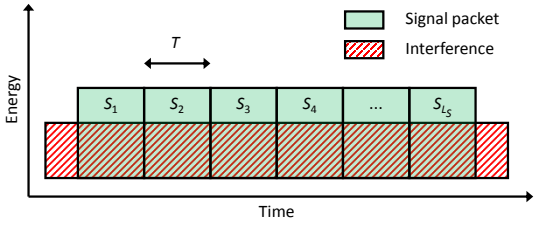

Fig. 4. PHY layer model from [4]

Finally, the SIR at the receiver, γ, is given by Eqn. 4.

$$\begin{aligned} \gamma_{dB} &= P^r_{S,dB} - P^{rf}_{I,dB} \\ \gamma &= 10^{\gamma_{dB}/10} \end{aligned} \quad (4)$$

D. PHY layer model

The PHY layer model is used to calculate the SER of the AWN as a function of the SIR at the receiver. We have adopted the basic PHY layer model from [4] and modified it for IEEE 802.15.4 and BLE. The signal is a packet of L_S symbols, each symbol of duration T, and the interference is continuous as shown in Fig. 4. All symbols are assumed to be transmitted through a common modulation scheme and code rate. The model could be extended to address different levels of robustness of the preamble and the data.

The model starts with the SER expression for the chosen modulation scheme in the presence of Additive White Gaussian Noise (AWGN). Next, the relationship between E_S/N_0 and Signal-to-Noise Ratio (SNR) at the receiver, and therefore SIR, is obtained. Finally, the E_S/N_0 term in the SER expression is replaced by the SIR.

1) IEEE 802.15.4 PHY model: The IEEE 802.15.4 2.4 GHz PHY employs O-QPSK modulation and Direct Sequence Spread Spectrum (DSSS) with bandwidth $B_S = 2$ MHz, chip rate $R_c = 2000$ kc/s, bit rate $R_b = 250$ kb/s and a codebook of $M = 16$ symbols [1]. For non-coherent demodulation, the SER, p, is given by Eqn. 5 [10].

$$p = 1/M \sum_{k=2}^{M} (-1)^k \binom{M}{k} e^{E_S/N_0(1/k-1)} \quad (5)$$

Assuming matched filtering at the receiver and half-sine wave pulse-shaping, we first calculate E_b/N_0.

$$E_b/N_0 = 0.625 \cdot R_c/R_b \cdot SNR = 5 \cdot SNR \quad (6)$$

where the DSSS process gain $R_c/R_b = 8$, $SNR = P^r_S/P^{rf}_N$, where P^r_S and P^{rf}_N are the signal and noise powers after the receiver filter. Then, we convert from E_b/N_0 to E_S/N_0.

$$E_S/N_0 = log_2(M) \cdot E_b/N_0 = 20 \cdot SNR \quad (7)$$

Following this, we replace the noise power occurring after the receiver filter with the equivalent interference power.

$$\begin{aligned} SNR = P^r_S/P^{rf}_N \leftarrow P^r_S/P^{rf}_I = \gamma \\ E_S/N_0 = 20\gamma \end{aligned} \quad (8)$$

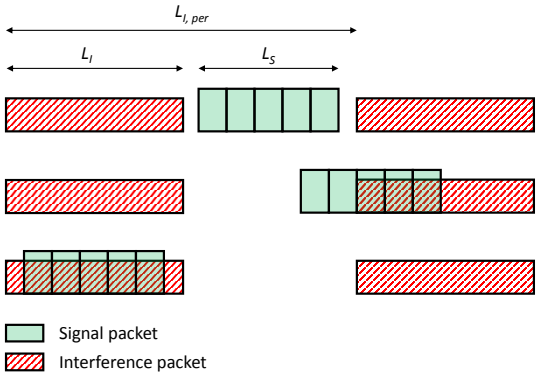

Fig. 5. Temporal model from [4]

Substituting for E_S/N_0 in Eqn. 5, the SER, p, as a function of SIR, γ, for IEEE 802.15.4 PHY is given by Eqn. 9.

$$p = 1/16 \sum_{k=2}^{16} (-1)^k \binom{16}{k} e^{20\gamma(1/k-1)} \tag{9}$$

2) BLE PHY model: The BLE PHY employs GFSK modulation with bandwidth $B_S = 1$ MHz, bit rate $R_b = 1$ Mb/s, $BT = 0.5$ and modulation index $h = 0.5$ [2]. For non-coherent demodulation, the SER, p, is given by Eqn. 10 [10].

$$p = 1/2 e^{-E_S/2N_0} \tag{10}$$

Following the steps used in the IEEE 802.15.4 PHY model, we calculate E_S/N_0 as a function of SIR, γ.

$$E_S/N_0 = E_b/N_0 = B_S/R_b \cdot SNR = SNR = \gamma \tag{11}$$

Substituting for E_S/N_0 in Eqn. 10, the SER, p, as a function of SIR, γ, for BLE PHY is given by Eqn. 12.

$$p = 1/2 e^{-\gamma/2} \tag{12}$$

E. Temporal model

The temporal model converts from SER to PER, taking the temporal aspects of both the signal and the interference into account. We have adopted the temporal model developed in [4]. The basic principle is to consider the probability of collision between signal packets and interference packets.

If X denotes the number of symbol collisions, then X is a random variable with probability mass function $f_X(x)$, where $x = 0, 1, ..., L_S$, where L_S is the length of the signal packet. The PER is then given by Eqn. 13 [4].

$$PER = \sum_{x=0}^{L_S} (1 - (1-p)^x) f_X(x) \tag{13}$$

where p is the SER.

The probability mass function, $f_X(x)$, depends on the length of the signal packet, L_S, the length of the interference packet, L_I, and the interference packet interval, $L_{I,per}$. We consider the signal and interference packets to be of fixed lengths and the interference packet interval to be fixed and of sufficient duration to accommodate the signal packet. Depending on the random position of the signal packet relative to the interference packet, three possible scenarios emerge, as shown in Fig. 5: no, partial, or full collision.

For fixed L_S and L_I, the probability mass function, $f_X(x)$, takes on the following generic form [4].

$$\begin{aligned} &f_X(0) = c_1 \\ &f_X(x) = c_2 \qquad\qquad x = 1, 2, ..., K-1 \\ &f_X(K) = c_3 \\ &f_X(x) = 0 \qquad x = K+1, K+2, ..., max(L_S, L_I) \end{aligned} \tag{14}$$

where c_1, c_2 and c_3 are constants, and K is the maximum number of symbol collisions given by $min(L_S, L_I)$.

Substituting for $f_X(x)$ in Eqn. 13 and simplifying, the PER as a function of the SER, p, is given by Eqn. 15 [4].

$$PER = c_2(Kp - 1 + (1-p)^K)/p + c_3(1 - (1-p)^K) \tag{15}$$

F. Results

Using the methodology described above, we perform a coexistence analysis between IEEE 802.15.4, BLE and IEEE 802.11b for the four network configurations listed in the methodology section. For each of the four network configurations, we study the effect of the following three parameters on the PER:

1) Interferer distance
2) Interferer packet interval
3) Interferer channel separation

In each of these three scenarios, we vary the network parameter of interest and fix the values of the remaining parameters. The fixed parameters in all three scenarios are as follows:

a) AWN parameters: $P_S^t = 0$ dBm, $D = 8$ m, $T = 16\mu$s (IEEE 802.15.4), 1μs (BLE), $L_S = 128$ bytes (IEEE 802.15.4), 40 bytes (BLE)
b) IWN parameters: $P_I^t = 0$ dBm (IEEE 802.15.4 and BLE), 20 dBm (IEEE 802.11b), $L_I = 128$ bytes (IEEE 802.15.4), 40 bytes (BLE), 1024 bytes (IEEE 802.11b)

The results of the coexistence analysis are shown in Fig. 6.

1) Interferer distance: In this scenario, the interferer distance from the receiver d is varied from 1 to 100 m. The interferer packet interval $L_{I,per}$ is fixed at 20 ms for IEEE 802.15.4 and BLE, and 10 ms for IEEE 802.11b. The transmitter and interferer channels are chosen as follows: IEEE 802.15.4 on channel 12 (2410 MHz), BLE on channel 3 (2410 MHz) and IEEE 802.11b on channel 1 (2412 MHz), thus constituting co-channel interference. All other parameters are fixed as specified earlier. The results are shown in Fig. 6a.

As Fig. 6a demonstrates, the BLE network is affected more by IEEE 802.15.4 interference than vice versa. The IEEE 802.15.4 network achieves 1% PER at a BLE interferer distance of around 7 m, whereas the BLE network requires an IEEE 802.15.4 interferer distance of around 17 m to achieve 1% PER. One reason for this difference is the DSSS process gain (around 9 dB) in the IEEE 802.15.4 network. Another reason is the longer channel-occupancy of IEEE 802.15.4

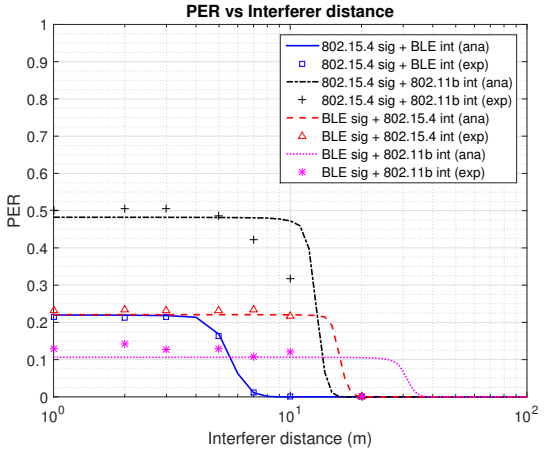

(a) Interferer distance

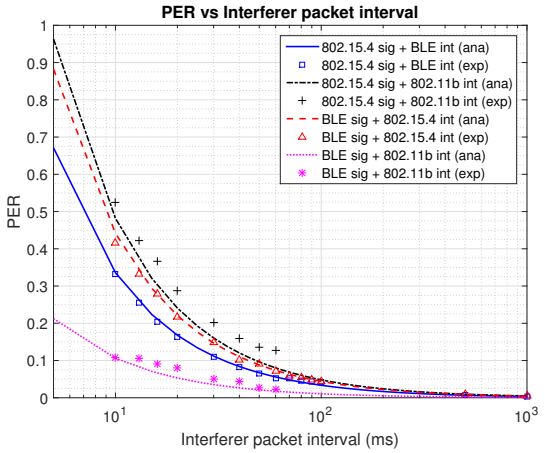

(b) Interferer packet interval

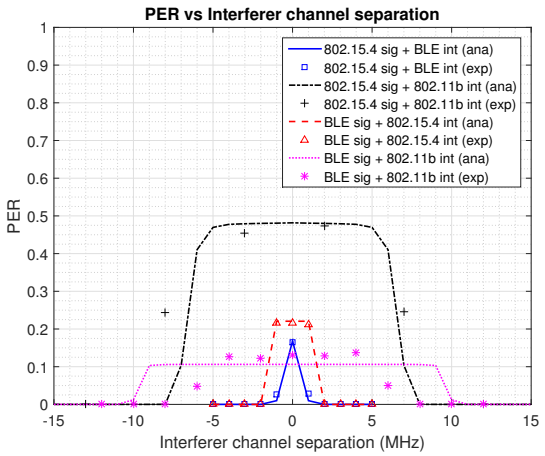

(c) Interferer channel separation

Fig. 6. Results of PHY layer coexistence analysis and experiments

packets (around 4 ms) compared to BLE packets (around 0.32 ms), thus causing the IEEE 802.15.4 interferer to affect the BLE network more.

It is also worth noting that, up to distances around 12 m, IEEE 802.11b interference affects the IEEE 802.15.4 network more than the BLE network. This is due to the shorter on-air time of BLE packets compared to IEEE 802.15.4 packets. This increases the likelihood that the BLE signal can avoid collision with the IEEE 802.11b interferer.

2) Interferer packet interval: In this scenario, the interferer packet interval $L_{I,per}$ is varied from 5 ms to 1 s. The interferer distance d is fixed at 5 m and and the transmitter and interferer channels are chosen as follows: IEEE 802.15.4 on channel 12 (2410 MHz), BLE on channel 3 (2410 MHz) and IEEE 802.11b on channel 1 (2412 MHz), thus constituting co-channel interference. All other parameters are fixed as specified earlier. The results are shown in Fig. 6b.

As Fig. 6b demonstrates, the BLE network is affected marginally more by the IEEE 802.15.4 network than vice versa. The IEEE 802.15.4 network achieves 10% PER at a BLE interferer packet interval of around 35 ms, whereas the BLE network achieves 10% PER at an IEEE 802.15.4 interferer packet interval of around 45 ms. The reasons for this difference are the DSSS process gain and the longer channel-occupancy of the IEEE 802.15.4 network, as discussed earlier.

Another observation is that the BLE network is affected much less (around 5 times) by IEEE 802.11b interference than by IEEE 802.15.4 interference, inspite of the higher transmit power of the IEEE 802.11b interferer (20 dBm) compared to IEEE 802.15.4 (0 dBm). There are two reasons for this. First, the IEEE 802.15.4 interferer has a higher channel-occupancy compared to the IEEE 802.11b interferer. Second, the IEEE 802.11b interference power scales down as the wideband IEEE 802.11b interference passes through the narrowband BLE receiver filter.

3) Interferer channel separation: In this scenario, the interferer channel separation from the transmitter is varied from -15 to 15 MHz, thus constituting adjacent channel interference. The interferer distance d is fixed at 5 m. The interferer packet interval $L_{I,per}$ is fixed at 20 ms for IEEE 802.15.4 and BLE, and 10 ms for IEEE 802.11b. All other parameters are fixed as specified earlier. The results are shown in Fig. 6c.

As Fig. 6c demonstrates, the BLE network is once again affected more by the IEEE 802.15.4 network than vice versa. At an interferer channel separation of 1 MHz, the BLE network has a PER of around 22%, whereas the PER of the IEEE 802.15.4 network drops to around 1%. At a 2 MHz channel separation, the PER drops to almost zero in both configurations. In case of IEEE 802.11b interference, both IEEE 802.15.4 and BLE networks get affected severely up to around 10 MHz channel separation, after which the PER drops down to almost zero.

IV. Experimental Study

To verify the results of the mathematical analysis, we perform experiments by setting up two networks, the AWN and the IWN. Each network consists of two wireless nodes, one transmitter (AWN Tx or IWN Tx) and one receiver (AWN Rx or IWN Rx). The experimental setup of the configurations with IEEE 802.15.4 or BLE interference is shown in Fig. 7a and with IEEE 802.11b interference is shown in Fig. 7b. For the wireless nodes of the IEEE 802.15.4 or BLE network,

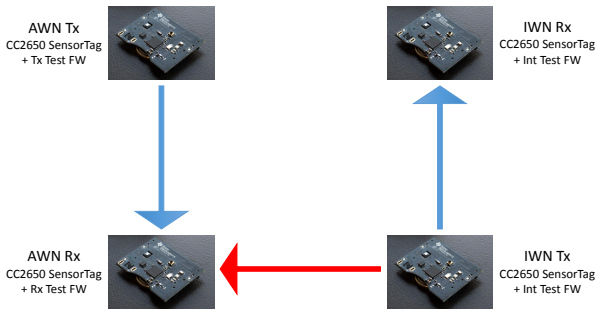

(a) IEEE 802.15.4 and BLE interference

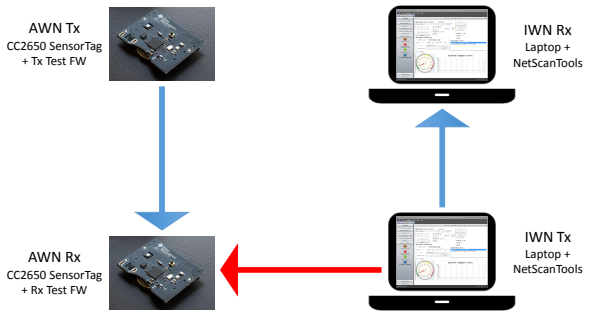

(b) IEEE 802.11b interference

Fig. 7. Setup for PHY and MAC layer coexistence experiments

we use the Texas Instruments SensorTag [11] based on the CC2650 multi-standard 2.4 GHz wireless micro-controller [12] that can operate in either IEEE 802.15.4 or BLE mode. For IEEE 802.11b interference, we set up an adhoc wireless network between two laptops and use the NetScanTools Pro Packet Flooder tool [13] to generate IEEE 802.11b traffic with specified parameters.

We study the coexistence of IEEE 802.15.4 and BLE with respect to the PHY layer parameters such as modulation scheme, data rate, bandwidth, packet size and packet interval. We further extend the experiments to the MAC layer to study the improvement in coexistence caused by mechanisms such as Carrier Sense Multiple Access (CSMA) and packet retransmissions in IEEE 802.15.4, and Adaptive Frequency Hopping (AFH) and packet retransmissions in BLE.

A. Experimental Setup for PHY Layer Coexistence Study

For the PHY layer coexistence experiments, we develop custom firmware on the Texas Instruments SensorTag using the PHY layer Application Programming Interfaces (APIs) for the CC2650 platform provided by Contiki OS [14]. Our custom firmware allows configuration of the PHY layer parameters of the IEEE 802.15.4 and BLE AWN and IWN such as transmit power, channel, packet length and packet interval. As mentioned earlier, IEEE 802.11b interference is generated using an adhoc network of two laptops running the NetScanTools Pro Packet Flooder tool. In each test case, we transmit packets at random time intervals from the AWN Tx to the AWN Rx and we transmit periodic interference packets from the IWN Tx to the IWN Rx. The PER is calculated based on the number of packets received correctly at the AWN Rx.

B. Experimental Setup for MAC Layer Coexistence Study

For the MAC layer coexistence experiments, we develop custom applications that run on top of the protocol stacks of IEEE 802.15.4 (TIMAC [15]) and BLE (BLE-stack [16]) provided by Texas Instruments. The applications allow configuration of the MAC layer parameters such as selecting beacon/non-beacon mode and enabling/disabling packet retransmission in IEEE 802.15.4, and configuring connection interval and channel map in BLE. In the IEEE 802.15.4 MAC, we select non-beacon mode, and enable acknowledgement with packet retransmission. In the BLE MAC, we set the connection interval to the desired packet interval, and configure the channel map with two channels, one overlapping with the selected IEEE 802.15.4 or IEEE 802.11b channel, and the other at least 20 MHz away. The IEEE 802.11b interference is generated as mentioned in the PHY layer coexistence study. The PER is calculated based on the number of retransmissions at the AWN Tx.

C. Results

We perform PHY layer coexistence experiments for all four network configurations and for all three parameter scenarios as mentioned in Section III. The PHY layer experimental results are shown in Fig. 6 alongside the PHY layer analytical results.

As Fig. 6 demonstrates, the experimental results match the analytical results with a Normalised Mean Square Error (NMSE) of around 0.78% for IEEE 802.15.4 and BLE interference. In the case of IEEE 802.11b interference, the NMSE is higher at around 11%.

Given the practical limitation on separating the coexisting networks in distance, particularly in indoor environments, we consider only packet interval and channel separation as parameters for the MAC layer coexistence experiments. The MAC layer experimental results are shown in Fig. 8 alongside the PHY layer analytical results.

As Fig. 8 demonstrates, the MAC layer mechanisms mentioned earlier lead to an improvement in coexistence performance. In all four network configurations, enabling packet retransmission improves reliability at the cost of increased latency. In order to retain reliability as the performance metric, we have calculated the PER based on the number of retransmissions.

The effect of CSMA in IEEE 802.15.4 is evident in case of IEEE 802.11b interference, where the reliability of IEEE 802.15.4 improves from the corresponding PHY layer scenario, e.g., PER drops from around 48% to around 33% at 10 ms interference packet interval. In the case of BLE interference, the BLE network hops between two channel. This results in reduced interference with the IEEE 802.15.4 network, making it difficult to observe the effect of CSMA separately. It is worth noting that BLE lacks a CSMA feature.

As expected, AFH in BLE results in improved reliability compared to the single-channel scenario considered in the

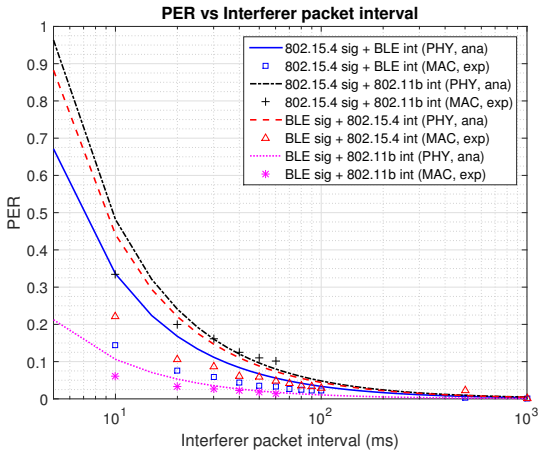

(a) Interferer packet interval

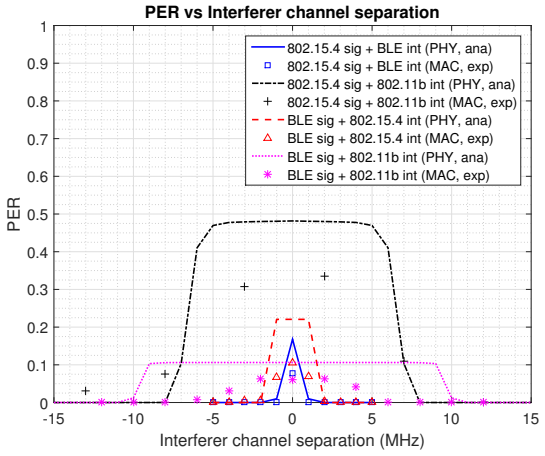

(b) Interferer channel separation

Fig. 8. Results of MAC layer coexistence experiments

PHY layer experiments. In the MAC layer experiments, the BLE network hops between two channels in both BLE as AWN and IWN scenarios. This results in reduced interference with the IEEE 802.15.4 network, indirectly improving the reliability by a factor of two. For instance, the PER of BLE as AWN drops from around 44% to around 22% at a 10 ms interference packet interval. This result can be extrapolated to a BLE channel map with a generic number of channels, provided adequate channel separation between the coexisting networks is guaranteed.

V. Discussion

Both IEEE 802.15.4 and BLE are designed for a variety of applications, such as safety and protection, industrial automation and process monitoring, with widely different data rate and latency requirements. This is evident from the supported BLE connection interval range (7.5 ms to 4 seconds) and the IEEE 802.15.4. beacon interval range (15.36 ms to 251.66 seconds). In this paper, we model the data rate using packet interval in both the PHY and MAC layers. Based on this, we study network reliability over a wide range of packet intervals (10 ms to one second). Our main findings are listed below:

1) At short interference packet intervals, e.g., 10 ms, the reliability of the AWN (IEEE 802.15.4 or BLE) is around 60%, when considering the PHY layer only. The MAC layer mechanisms such as AFH in BLE, and CSMA as well as packet retransmission in IEEE 802.15.4, improve the reliability to around 85%.
2) In order to study applications with lower data rates, we increase the interference packet interval to 20 ms, then 50 ms, then all the way to one second. The reliability of the AWN increases steadily as a result, e.g., 80% at 20 ms, 93% at 50 ms and 99% at one second.
3) In a real deployment of a dense network, with 10 to 100 nodes installed in the same transmission range, i.e., 30 to 50 m, the data rate of a single node could be much more than 10 ms, e.g., 1 second. However, the entire IWN can be considered as a single interfering node with a higher data rate (10 to 100 times more than a single node), thereby decreasing the reliability of the AWN.
4) In the case of IEEE 802.11 interference, the reliability of the AWN is around 95%, 50% and 5% at an IEEE 802.11 traffic load of 1%, 10% and 20% respectively. This is a significant decrease in reliability and necessitates a coexistence solution.

VI. Conclusion

This paper has described a systematic study of coexistence between IEEE 802.15.4, BLE and IEEE 802.11b in the unlicensed 2.4 GHz ISM band. First, we performed a mathematical analysis and quantified the effect of varying the spatial, temporal and frequency parameters of the interference on the reliability of the network. We compared the resilience of the PHY layers of the aforementioned technologies against cross-technology interference. Then, we set up experiments with real wireless networks and verified our analytical results. Finally, we extended the experiments to the MAC layer to study the effect of MAC layer mechanisms on coexistence performance.

In general, we found that BLE is affected more by IEEE 802.15.4 interference than vice versa. This could be attributed to the DSSS process gain and longer channel-occupancy of IEEE 802.15.4 compared to BLE. On the other hand, we found that BLE is more resilient than IEEE 802.15.4 against IEEE 802.11 interference. This is mainly due to BLE's shorter channel-occupancy than IEEE 802.15.4, which exposes it less to IEEE 802.11 interference.

In order to connect this study to real-world applications, we have provided a basis to map different applications, based on their QoS requirements, to different regions of the reliability vs. interferer packet interval curve. Such a mapping helps to identify regions of interest that require a coexistence solution. Furthermore, the study of reliability vs. interferer channel separation could be useful in developing a frequency-domain cooperative coexistence solution.

VII. Scope for Future Work

In this paper, we have considered a simple geometric configuration with each network consisting of two nodes. This could be extended to a more complex configuration to study more realistic networks. In the PHY layer model, we have assumed the packet to be homogeneous in robustness. While this conservative model performs accurately at low SIR, it could be extended to address the different levels of robustness of the data and the preamble portion of the packets.

References

[1] "IEEE Standard for Local and metropolitan area networks - Part 15.4: Low-Rate Wireless Personal Area Networks (LR-WPANs)," *IEEE Std 802.15.4-2011*, 2011.

[2] "Bluetooth Specification Version 4.2," *Core Version 4.2*, 2014.

[3] "IEEE Standard for Information technology - Telecommunications and information exchange between systems - Local and metropolitan area networks - Specific requirements Part 11: Wireless LAN Medium Access Control (MAC) and Physical Layer (PHY) Specifications," *IEEE Std 802.11-2012*, 2012.

[4] S. J. Shellhammer, "Estimation of Packet Error Rate Caused by Interference using Analytic Techniques - A Coexistence Assurance Methodology," *IEEE P802.19 Wireless Coexistence*, 2005.

[5] "Bluetooth Specification Version 2.1 + EDR," *Core Version 2.1 + EDR*, 2007.

[6] "IEEE Recommended Practice for Information technology - Local and metropolitan area networks - Specific requirements - Part 15.2: Coexistence of Wireless Personal Area Networks with Other Wireless Devices Operating in Unlicensed Frequency Bands," *IEEE Std 802.15.2-2003*, 2003.

[7] R. G. Garroppo, L. Gazzarrini, S. Giordano, and L. Tavanti, "Experimental assessment of the coexistence of WiFi, ZigBee, and Bluetooth devices," *IEEE International Symposium on a World of Wireless, Mobile and Multimedia Networks (WoWMoM)*, pp. 1–9, 2011.

[8] S. Silva, T. Fernandes, A. Valente, and A. Moreira, "Coexistence and Interference Tests on a Bluetooth Low Energy Front-End," *IEEE Science and Information Conference (SAI)*, pp. 1014 – 1018, 2014.

[9] J. Wyffels, J.-P. Goemaere, B. Nauwelaers, and L. de Strycker, "Influence of Bluetooth Low Energy on WiFi Communications and Vice Versa," *European Conference on the Use of Modern Information and Communication Technologies*, vol. 302, pp. 205–216, 2014.

[10] "Coexistence analysis of IEEE Std 802.15.4 with other IEEE standards and proposed standards," *IEEE P802.15 Wireless Personal Area Networks*, 2010.

[11] "SimpleLink Multi-standard SensorTag." [Online]. Available: http://www.ti.com/sensortag

[12] "CC2650 SimpleLink multi-standard 2.4 GHz ultra-low power wireless MCU." [Online]. Available: http://www.ti.com/product/CC2650

[13] "NetScanTools internet and network information toolkits for Windows." [Online]. Available: http://www.netscantools.com

[14] "Contiki: The Open Source OS for the Internet of Things." [Online]. Available: http://www.contiki-os.org/

[15] "IEEE802.15.4 Medium Access control (MAC) software stack." [Online]. Available: http://www.ti.com/tool/timac

[16] "Bluetooth low energy software stack." [Online]. Available: http://www.ti.com/tool/ble-stack